Extensional collapse of the Tibetan Plateau: Results of three-dimensional finite element modeling

Mian Liu and Youqing Yang

Department of Geological Sciences, University of Missouri-Columbia, Columbia, Missouri, USA

Received 17 October 2002; revised 7 April 2003; accepted 12 May 2003; published 1 August 2003.

[1] Following their initial collision 50–70 Myr ago, the Indian and Eurasian plates have been continuously converging toward each other. Whereas the regional stress field is predominately compressive, the Late Cenozoic tectonics within the Tibetan Plateau features widespread crustal extension. Numerous causes of the extension have been proposed, but their relative roles remain in debate. We have investigated the major factors contributing to the Tibetan extension in a three-dimensional viscoelastic model that includes both lateral and vertical variations of lithospheric rheology and relevant boundary conditions. Constrained by the present topography and GPS velocity field, the model predicted predominately extensional stress states within the plateau crust, resulting from mechanical balance between the gravitational buoyancy force of the plateau and the tectonic compressive stresses. The predicted stress pattern is consistent with the earthquake data that indicate roughly E-W extension in most of Tibet and nearly N-S extension near the eastern margin of the Tibetan Plateau. We explored the parameter space and boundary conditions to examine the stress evolution during the uplift of the Tibetan Plateau. When the plateau was lower than 50% of its present elevation, strike-slip and reverse faults were predominate over the entire plateau, and no E-W crustal extension was predicted. Significant crustal extension occurs only when the plateau has reached ~75% of its present elevation. Basal shear associated with underthrusting of the Indian plate beneath Tibet may have enhanced crustal extension in southern Tibet and the Himalayas, and a stronger basal shear during the Miocene may help to explain the development of the South Tibetan Detachment System. *INDEX TERMS:* 7209 Seismology: Earthquake dynamics and mechanics; 8109 Tectonophysics: Continental tectonics—extensional (0905); 8102 Tectonophysics: Continental contractional orogenic belts; 8164 Tectonophysics: Stresses—crust and lithosphere; 9604 Information Related to Geologic Time: Cenozoic; *KEYWORDS:* Tibetan Plateau, extension, finite elements, stress, continental collision, gravitational collapse

Citation: Liu, M., and Y. Yang, Extensional collapse of the Tibetan Plateau: Results of three-dimensional finite element modeling, *J. Geophys. Res.*, *108*(B8), 2361, doi:10.1029/2002JB002248, 2003.

1. Introduction

[2] The Himalayan-Tibetan Plateau, the largest mountain belt on Earth today, has resulted mainly from the continued Indian-Eurasian plate convergence following their initial collision about 50–70 Myr ago [*Yin and Harrison*, 2000]. Whereas geological records [*DeMets et al.*, 1994] and space geodetic measurements [*Larson et al.*, 1999; *Paul et al.*, 2001; *Wang et al.*, 2001] show continuing northward movement of the Indian plate relative to stable Eurasia at a rate of 35–50 mm yr^{-1}, evidence from Landsat imagery, fault plane solutions of earthquakes, and field observations indicates that, for the past 10 Myr or so, the Tibetan Plateau has experienced widespread extension as indicated by the roughly north trending rifts in Tibet [*Armijo et al.*, 1986; *Blisniuk et al.*, 2001; *Mercier et al.*, 1987; *Molnar and Tapponnier*, 1977; *Ni and York*, 1978; *Yin et al.*, 1999] (Figure 1).

0148-0227/03/2002JB002248$09.00

[3] The cause of the Tibetan extension and its relationship to the rise and fall of the Tibetan Plateau are of fundamental importance to continental tectonics; they also bear profound implications for climate change [*Guo et al.*, 2002; *Kutzbach et al.*, 1989; *Molnar et al.*, 1993; *Ruddiman and Kutzbach*, 1989; *Zhisheng et al.*, 2001]. Whereas numerous causes of the Tibetan extension have been proposed, their relative roles are debated. One common explanation for the Tibetan crustal extension is gravitational collapse, driven by excess gravitational potential energy (GPE) arising from the buoyant crustal root and the upwelled asthenosphere [*Chen and Molnar*, 1983; *Dewey*, 1988; *England and Houseman*, 1989; *Molnar and Lyon-Caen*, 1988]. Conceptually, it is easy to show that a plateau in isostatic equilibrium may be gravitationally unstable, and the lateral gradient of the GPE tends to spread the plateau toward the surrounding lowland [*Artyushkov*, 1973; *England and Molnar*, 1997; *Molnar and Lyon-Caen*, 1988]. However, England and coworkers' thin-viscous-sheet model, while capturing many basic features of continental deformation in Tibet and surrounding regions,

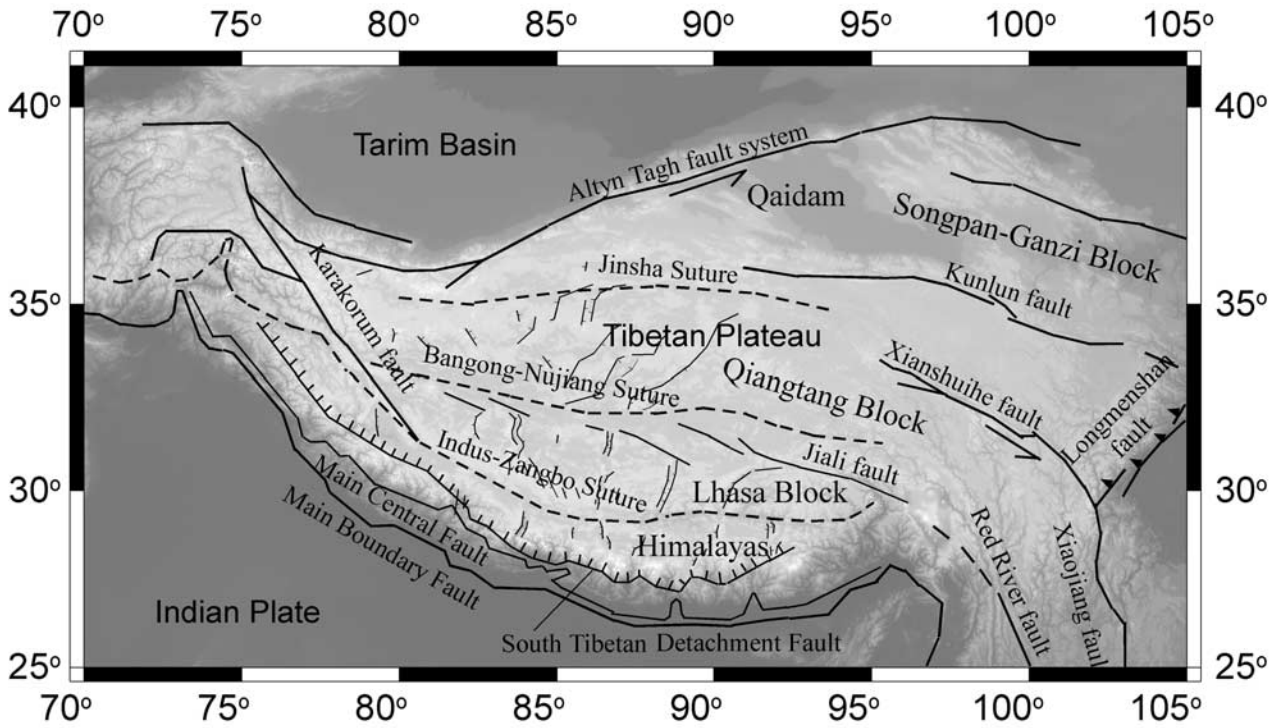

Figure 1. Topographic relief (background) and simplified tectonic map of the Himalayan-Tibetan Plateau and sounding regions. Tick marks indicate normal faults [after *Yin*, 2000].

failed to reproduce the E-W extension that dominates the present deformation of Tibet [*England and Houseman*, 1986, 1988; *Houseman and England*, 1996]. Their explanation is that convective removal of the lower part of the mantle lithosphere under the Tibetan Plateau, not included in their thin-viscous-sheet model, may have provided the excessive GPE needed to cause the E-W extension. Using the similar thin-viscous-sheet approximation of the Eurasian continent and incorporating topography and strain rate data, *Flesch et al.* [2000] were able to predict E-W extensional stresses in Tibet that results from excessive GPE of the plateau. However, their results predict strongest E-W extension in the northern and northwestern parts of the Tibetan plateau, whereas both earthquake data and rift development indicate that the E-W extension has been most active in southern Tibet (Figure 1). Because the thin-viscous-sheet models solve for vertically averaged deviatoric stresses, they cannot be used to investigate vertical variations of lithospheric rheology and stress states, which have been suggested as critical for understanding the evolution of the Tibetan Plateau [*Bird*, 1991; *Royden*, 1996; *Yin*, 2000; *Zhao and Morgan*, 1987].

[4] Because the E-W extension is best developed in southern Tibet and the Himalayas [*Armijo et al.*, 1986; *Ratschbacher et al.*, 1994; *Tapponnier et al.*, 1981] (Figure 1), other workers argued that the formation of the Tibetan rifts was due to local boundary conditions, such as oblique convergence or basal shear associated with subduction of the Indian plate under Tibet, that caused radial expansion and stretching along the Himalayan arc [*Armijo et al.*, 1986; *McCaffrey and Nabelek*, 1998; *Ratschbacher et al.*, 1994; *Seeber and Pecher*, 1998]. However, recent field work has revealed extensive normal faults in northern Tibetan Plateau [*Blisniuk et al.*, 2001; *Yin et al.*, 1999]. These normal faults may be kinematically linked to the north trending rifts in southern Tibet [*Yin*, 2000]. By comparing the spatial and temporal development of the Tibetan rifts with other Cenozoic rifts in eastern Asia, *Yin* [2000] argued for a common cause in a regional extensional stress field perhaps related to tectonic boundary conditions in eastern Asia.

[5] All the factors discussed in the previous studies may have contributed to the crustal extension in the Tibetan Plateau. What remain uncertain are the relative roles of these factors in the Tibetan extension and in the rise and fall of the Himalayan-Tibetan Plateau. It is clearly desirable to have a self-consistent geodynamic model where all the major factors contributing to the Tibetan extension can be evaluated. We have developed a three-dimensional (3-D) finite element model to explore the relative roles of GPE, rheologic structure, basal shear, local boundary conditions, and regional tectonic boundary conditions in the crustal extension of the Tibetan Plateau. Constrained by the present-day topography, plate boundary conditions, and kinematic data, the model successfully reproduced the major stress pattern within the Tibetan crust as indicated by the earthquake data. We then explored the major parameters and boundary conditions that may have significantly changed during the Tibetan orogenesis to investigate the mechanics that controls the rise and fall of the Himalayan-Tibetan Plateau.

2. Numerical Model

[6] Figure 2 shows the geometry and boundary conditions of our finite element model based on the present

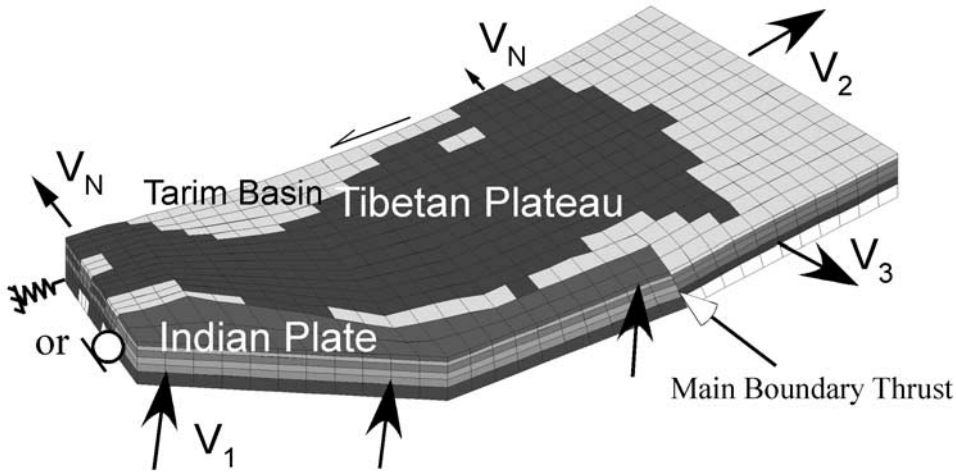

Figure 2. Geometry and general boundary conditions of the finite element model. The Main Boundary Thrust, used in the model in a general sense to represent the thrust fault system between the Indian and Eurasian plates, is simulated by a weak zone. The effective viscosity of this weak zone can be adjusted to simulate mechanical coupling between the Indian plate and the Asian continent. Six layers of elements are used to approximate the rheological variations between the Indian plate, the Tibetan Plateau, and the rest of the Asian continent (Figure 3). The details of boundary conditions are discussed in the text. See color version of this figure in the HTML.

tectonic setting of the Himalayan-Tibetan Plateau. The model includes a rigid Indian plate colliding with a relatively weak Eurasian continent. The dynamic coupling between these two plates is through a fault zone simulating the Main Boundary Thrust (MBT) (Figure 1). The Indian plate moves at N20°E with a constant velocity relative to stable Eurasia [*DeMets et al.*, 1994]. On the eastern and southeastern sides of the model, either displacement or stress boundary conditions are assigned to simulate the observed lateral crust extrusion from the collision zone as suggested by geodetic data [*Chen et al.*, 2000; *Larson et al.*, 1999; *Wang et al.*, 2001]. On the western side, either the roller or the spring elements are used to simulate the lateral resisting force of the Pamir Plateau. On the northern side we used either a velocity boundary based on the GPS data or the spring elements to approximate the resistance from the Tarim block. In most cases we also applied a small (5 MPa) shear stress along the northern side of the model domain to simulate the effects of the left-lateral strike-slip motion along the Altyn Tagh fault and other faults in the region. The top surface approximates the real topography base on the digital topographic data (National Geophysics Data Center, Global 1.0), and the topographic loading is included explicitly in the model by calculating the weight of rock columns in each surface grid of the finite element model. Given the uncertainty of the deep structures under the plateau, we choose the bottom of the model to be at 70 km depth, and use the Winkler spring mattress [*Desai*, 1979] to simulate isostatic restoring force [*Williams and Richardson*, 1991]. Under the assumption of isostasy, the deviatoric stresses within the upper crust, our main focus here, are not strongly affected by variations of the isostatic compensation depth (or crustal thickness) as long as the proper isostatic rebounding force is applied at the bottom. This is especially true when a weak lower crust is present [*Liu et al.*, 2000a].

[7] The model assumes the linear viscoelastic (Maxwell) rheology. Although the long-term deformation of the lithosphere is probably closer to that of a power law fluid, with the strain rate being proportional to the cubic power of stress [*Brace and Kohlstedt*, 1980; *Kirby and Kronenberg*, 1987], the linear (Newtonian) viscosity is acceptable for first-order approximation, especially when our focus here is the spatial pattern, rather than the absolute magnitude, of the deviatoric stresses. The first-order lateral rheological variations are represented by a stiff Indian plate, a weak Tibetan Plateau (defined by the 3000-m contour in the model, see Figure 2), and the rest of the Eurasia continent with rheologic values in between. The vertical rheologic variations of these blocks are represented in the model by six layers of material with different effective viscosity (Figure 3). The Young's modulus and Poisson ratio used in the model are 7×10^{10} Pa and 0.25, respectively. The density of the crust and the upper mantle are taken to be 2800 and 3300 kg m^{-3}, respectively. Other specific parameter values are given when the numerical experiments are presented.

[8] The present state of deviatoric stresses within the Tibetan Plateau results from the mechanical balance between the tectonic compression from the indenting Indian plate and the gravitational buoyancy force of the plateau, as well as resisting forces around and at the base of the plateau. The general mechanical equilibrium can be written as

$$\frac{\partial \sigma_{ij}}{\partial x_j} + \rho g_i = 0; \qquad i,j = 1,2,3, \tag{1}$$

where σ_{ij} is the stress tensor, ρ is the density, and $g_i = (0, 0, g)^T$ is the vector of gravitational acceleration. The equation is solved using the finite element method. We built the numerical codes using the commercial finite element package FEPG 3.0 (www.fegensoft.com/english/

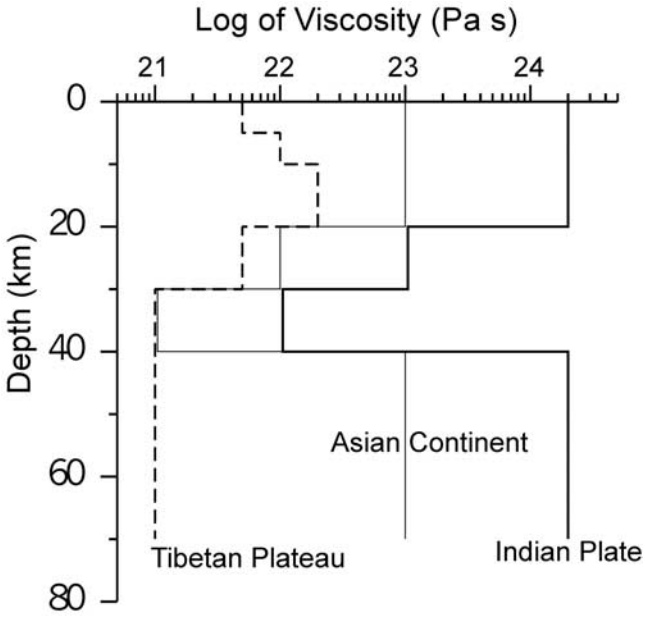

Figure 3. The effective viscosity profiles for the Tibetan Plateau (dashed line), the Indian plate (thick line), and the rest of the Asian continent (thin line) used in this work. Other values were used in the numerical experiments to explore the effects of rheologic structures. See text for details.

index.htm), and tested the codes against results of the analytic solutions of numerous simple problems and those of TECTON for simple 3-D problems [*Liu et al.*, 2000a]. We used the Goodman joint elements to simulate the MBT fault [*Goodman et al.*, 1968]. The model fault zone is a 20-km-thick weak zone with a dip of 35°. The viscosity of the fault zone can be adjusted to simulate different degrees of mechanical coupling between the Indian and the Asian plates. For simulations of active tectonics, the rheology of the MBT is adjusted to match the surface velocity change across the MBT as indicated by the GPS data (Figure 4).

3. Active Crustal Extension in Tibet

[9] We started the numerical experiments with simulations of the active Tibetan tectonics because of the relatively good constraints. Figure 4 shows the topography and the GPS velocities of the Tibetan Plateau and surrounding regions, and Figure 5 shows the earthquake focal mechanisms indicating the active E-W crustal extension in Tibet. To examine the possible causes of the Tibetan extension, we systematically evaluate the effects of all major factors proposed in previous studies. We started with the evaluation of gravitational collapse because the excess GPE of the Himalayan-Tibetan Plateau relative to the surrounding lowland is better constrained than other factors that may have contributed to the Tibetan extension

$$\Delta\mathrm{GPE} = \int_{-h}^{z} \Delta\rho g z dz, \qquad (2)$$

where h is the elevation of the plateau above the reference lowland, z is the depth, $\Delta\rho$ is the density contrast between the plateau and the lowland at depth z, and g is the gravitational acceleration. For a plateau in Airy isostasy, ΔGPE is equivalent to the extensional force (per unit length) of the plateau on the surrounding lowland, or sometimes called the gravitational buoyancy force of the plateau [*Flesch et al.*, 2000; *Liu and Shen*, 1998; *Molnar and Lyon-Caen*, 1988]. With the further assumption of a uniform crustal density, ΔGPE can be directly related to topographic loading of the plateau. In our model the topographic loading is calculated using the digital topography.

[10] The first step in our numerical investigation is to see whether the ΔGPE of the Himalayan-Tibetan Plateau could explain the observed stress state within the Tibetan crust for the present topography and kinematic boundary conditions.

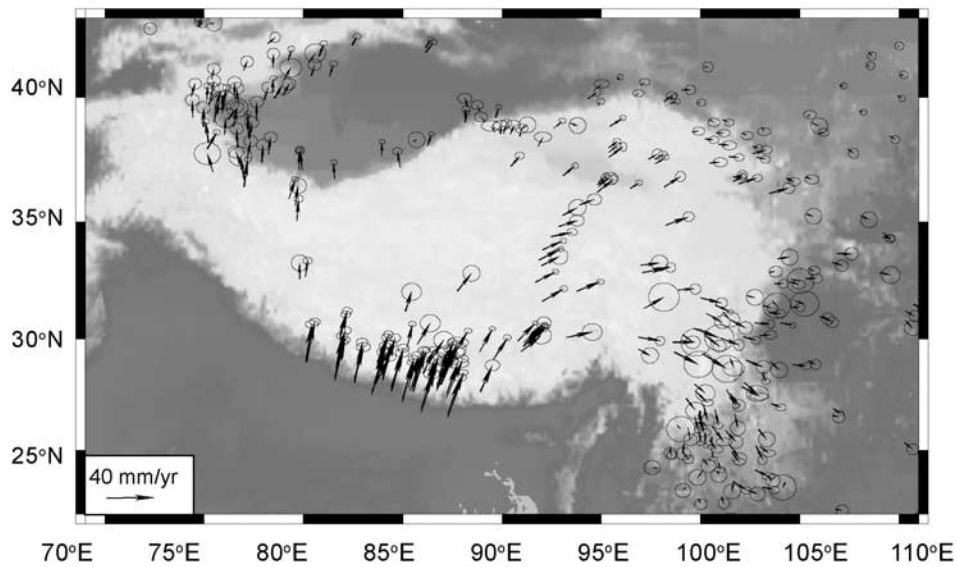

Figure 4. The GPS velocity field relative to stable Siberia (data from *Chen et al.* [2000], *Larson et al.* [1999], and *Wang et al.* [2001]). Error ellipses are for 95% confidence. Velocity scale is shown in the lower left corner. See color version of this figure in the HTML.

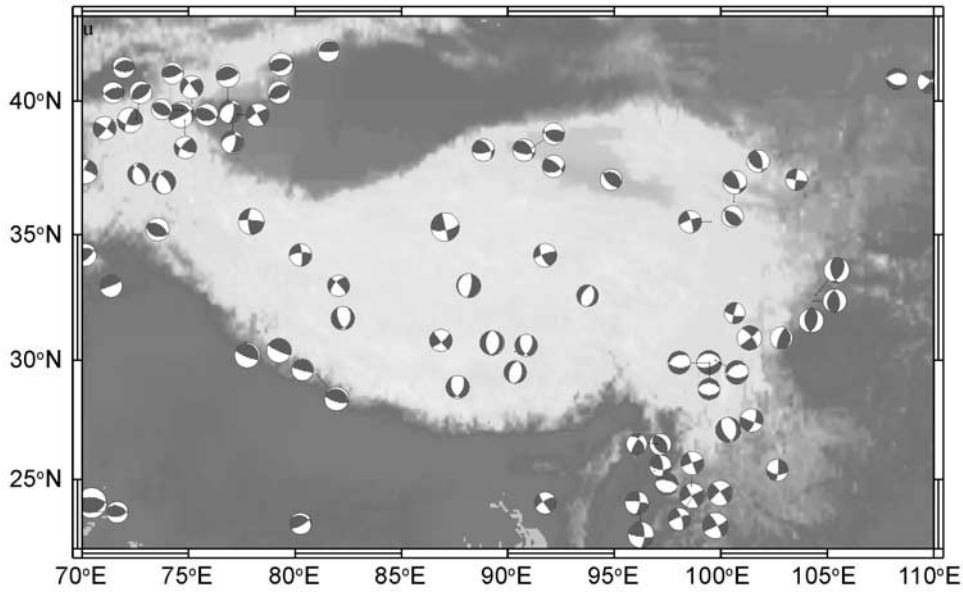

Figure 5. Earthquake focal mechanisms showing predominant E-W crustal extension. Data are events with magnitude >5.5 and depth <33 km from the Harvard catalog (from 1976 to 2000). See color version of this figure in the HTML.

Figure 6 shows the predicted crustal stresses using the velocity boundary conditions based on the GPS data: a uniform 44 mm yr^{-1} convergence in the direction of N20°E along the Himalayan front (V_1 in Figure 2), 7 mm yr^{-1} eastward velocity on the east side (V_2 in Figure 2), and 10 mm yr^{-1} on the southeastern side of the model (V_3 in Figure 2). The convergence rate used here is somewhat arbitrary, partly because the convergence rate varies along the Himalayan front, and the rate indicated by the recent GPS data (~35 mm yr^{-1} [*Paul et al.*, 2001]) is lower than the long-term averaged convergence rate (~50 mm yr^{-1} [*DeMets et al.*, 1994]). The effects of convergence rate are discussed below. On the northern side of the model domain, we used a northward velocity of 20 mm yr^{-1} at the western end and decreased it linearly to zero at the eastern end. This is to reflect the variation of the GPS velocities along the northern margin of the Tibetan Plateau (Figure 4), although using a uniform zero northward velocity on this boundary produced similar results. The roller elements are used on the western side to prohibit motion normal to that boundary.

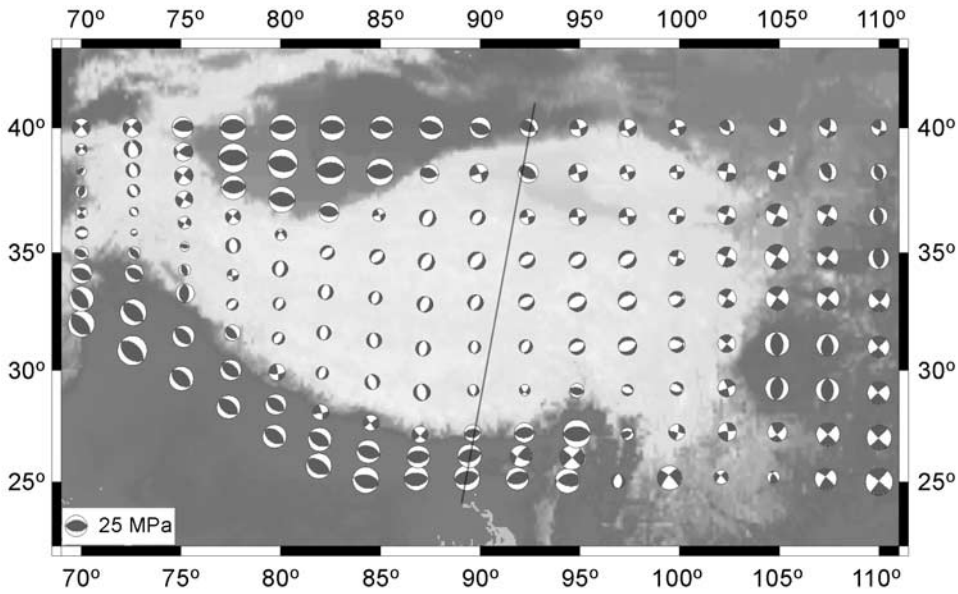

Figure 6. Predicted deviatoric stresses in the upper crust (at 10 km depth) of the Tibetan Plateau and surrounding regions. The three-dimensional stress state at each node is shown using lower hemisphere stereonet projection similar to that for earthquake focal mechanisms. Stress scale is shown in the lower left corner. The line indicates the location of the profile in Figure 8. See color version of this figure in the HTML.

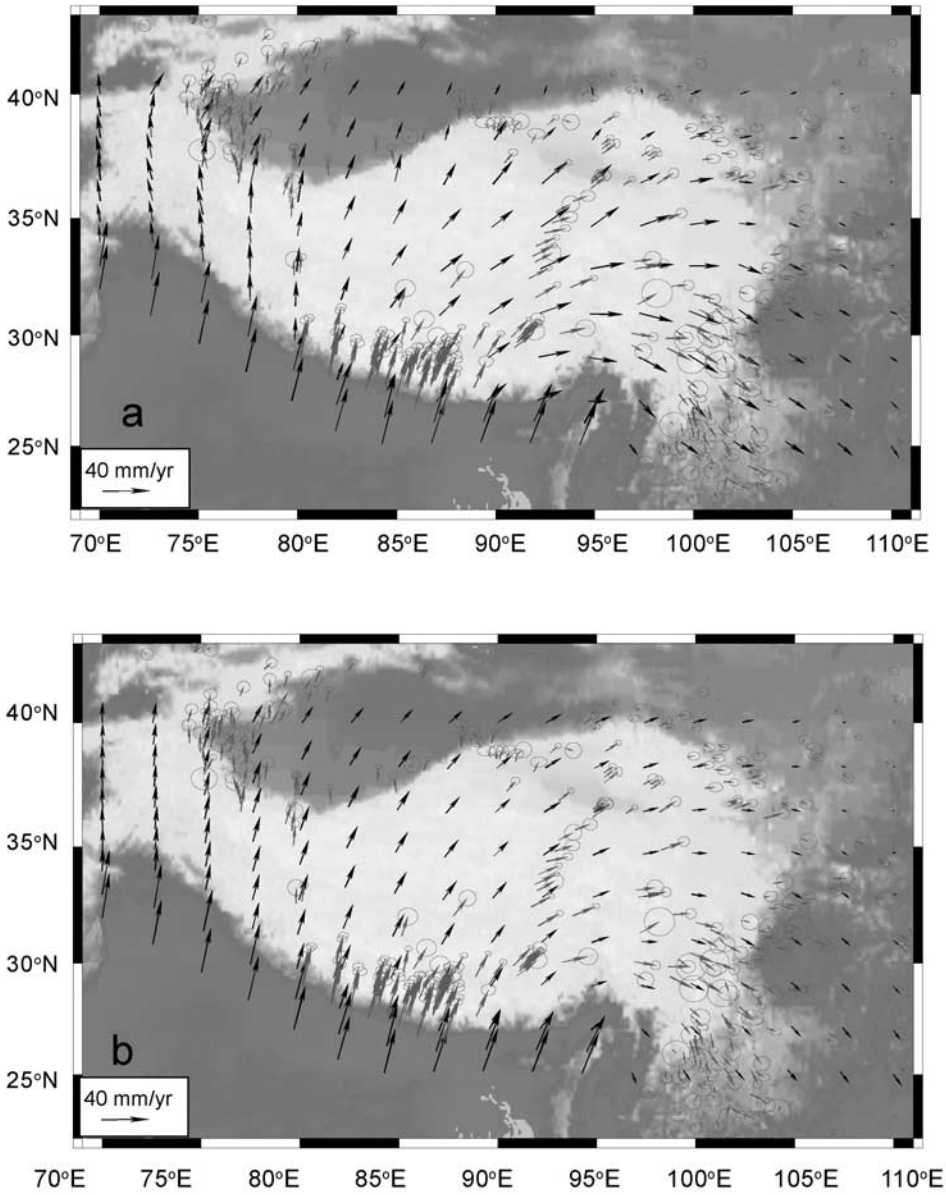

Figure 7. Comparison of the predicted surface velocity (arrows) and GPS measurements (arrows with error ellipses). All velocities are relative to stable Eurasia. (a) The same case as in Figure 6. Note the high velocities in eastern Tibet and high velocity gradient across the eastern margin of the plateau. (b) A high viscosity (10^{25} Pa s) for the upper Tibetan crust was used to simulate short-term deformation that may be more proper for comparison with the GPS data. See color version of this figure in the HTML.

[11] A comparison with Figure 4 shows significant similarity between the predicted deviatoric stresses and the stress pattern indicated by earthquake fault plane solutions, including the dominantly extensional stresses in Tibet. The predicted extensional direction is roughly E-W in southern and central Tibet, which changes to nearly N-S around the southeastern margin of the Tibetan Plateau, consistent with the earthquake data. Note that the stresses in Figure 6 are the steady state, background deviatoric stresses. The transient stress changes during the cycles of stress accumulation and release by earthquakes or aseismic slips are not included, because they are relatively small compared to the background stresses, and because they are difficult to simulate for the large spatial scale considered here. The geological structures and the general patterns of earthquake focal mechanisms reflect mainly the background deviatoric stresses, which depend on the driving forces, boundary conditions, and rock rheology. We simulated the steady state background stresses by using viscosities in the range appropriate for long-term geological deformation (10^{22}–10^{23} Pa s [see *England and McKenzie*, 1982; *Flesch et al.*, 2001]). Starting with the elastic solution, we ran the models much longer than the Maxwell relaxation time, which is about 3000 years for the chosen elastic moduli and viscosities, until the initial stresses were largely relaxed and a steady state stress field was achieved [*Liu et al.*, 2000a].

[12] Figure 7a shows the predicted surface velocity field for the same case shown in Figure 6. The results are

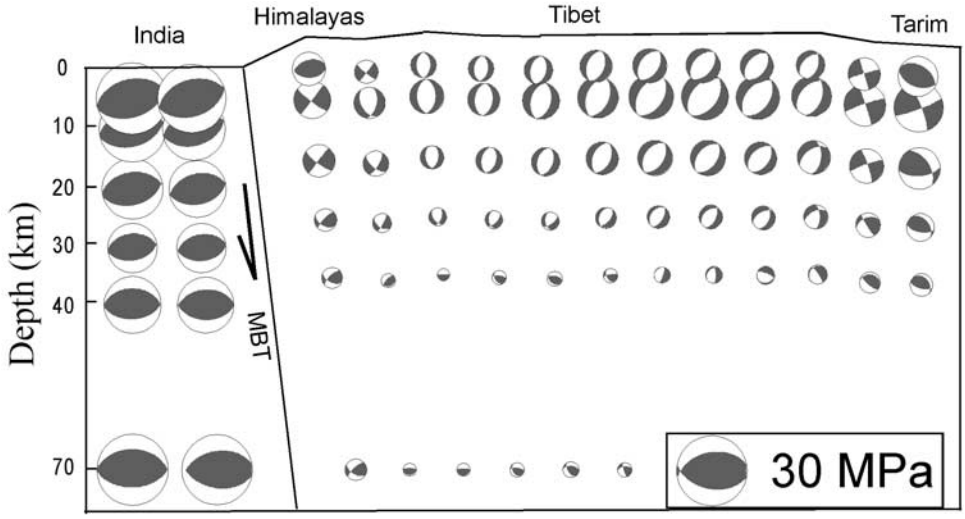

Figure 8. Vertical profile of the predicted deviatoric stresses for the case shown in Figure 6. Each symbol shows the lower hemisphere stereonet project of the three-dimensional stress state as in Figure 6. The depth variation of the magnitude of stresses under Tibet is related to the rheological structures used in the model (Figure 3). The stress scale is shown in the lower right corner. See color version of this figure in the HTML.

generally comparable to the GPS data. Some of the discrepancies are due to the simplified velocity boundary conditions used in the model. However, note that the predicted velocities in the eastern part of the plateau are significantly higher than the GPS velocities. This is partly explained by the timescale-dependent rock rheology [*Liu et al.*, 2002, 2000b]. The rheologic structure used here (Figure 3) is proper for long-term crustal deformation; in this case gravitational spreading of the plateau is significant, resulting in the high velocity gradients near the eastern margin of the Tibetan Plateau in Figure 7a. Over short timescales that are pertinent to GPS measurements (typically a few years), the crustal rheology may be closer to elastic. Using a high viscosity (10^{25} Pa s) to simulate the near-elastic short-term crustal deformation, the model predicted a somewhat better fit to the GPS velocities (Figure 7b). Internal faults, however, would further complicate the velocity field because crust motion is mainly along the fault zones. The similarity between the GPS velocity field in Tibet and the prediction of long-term gravitational spreading may be explained by block motion along numerous strike-slip faults aligned along the ''flow lines'' of the spreading plateau, a condition not found in all orogens [*Liu et al.*, 2000b]. Because the model does not include the strike-slip faults in Tibet and the current GPS data within the Tibetan Plateau are sparse, the comparison of model results with the GPS data should be taken with caution.

[13] The results in Figures 6 and 7 may impose some useful constraints on the lithospheric rheology of the plateau relevant for deformation at geological timescales. For the present kinematic boundary conditions and elevation, we found that the average effective viscosity for the Tibetan crust needs to be in the range between 10^{21} and 10^{22} Pa s for the observed active E-W extension to occur in the plateau. Such a weak Tibetan crust is consistent with results of other models and estimations [*England and Molnar*, 1997; *Flesch et al.*, 2001]. There is a tradeoff between the Tibetan rheology and the convergence rate, or more accurately, the mechanical coupling between the Indian and Eurasian plates. In the model this coupling is simulated by adjusting the rheology of the MBT zone to match the velocity field across the plate boundary. In Figures 6 and 7a, relatively weak MBT is used to reproduce a large velocity drop over the Himalayan front as indicated by the GPS results of *Larson et al.* [1999]. Recent GPS data show a more gradual velocity gradient across the Himalayas and over the entire Tibetan Plateau [*Wang et al.*, 2001], indicating strong coupling, or locking, between the two plates during the period of the GPS measurements. A long-term strong coupling between the Indian and Eurasian plates would require an even weaker Tibetan crust than that assumed in Figure 6 to account for the continuous E-W extension in the past 10 Myr or so. On the other hand, a drop by a factor of 5 of the Tibetan crustal viscosity shown in Figure 3 would lead to prediction of collapse of the entire plateau at unreasonably high rates (>40 mm yr^{-1}).

[14] Figure 8 shows the depth variation of the predicted stresses for the same case as in Figure 6. As in Figure 6, the symbols show the 3-D stress states at each node using the lower hemisphere projection, although here the stress projections are viewed at different depths. The stresses indicate predominately N-S compression within the Indian plate. The change of the magnitude of the stresses with depth reflects the depth-dependent rheology (Figure 3). Over the high plateau the stresses are characterized by roughly E-W extension in the upper crust, whereas in the lesser Himalayas and the northern rims of the plateau, the stress states are predominantly compressive or strike slip. The prediction of extension to be largely limited to the upper crust of Tibet is consistent with earthquake data [*Molnar and Chen*, 1983]. However, a number of deep (>75 km) normal-faulting earthquakes occurred under southern Tibet and the Himalayas [*Chen and Kao*, 1996]. Because gravitational collapse is normally expected to occur only within the crust [*Bird*, 1991; *Liu and Shen*, 1998], these deep normal events

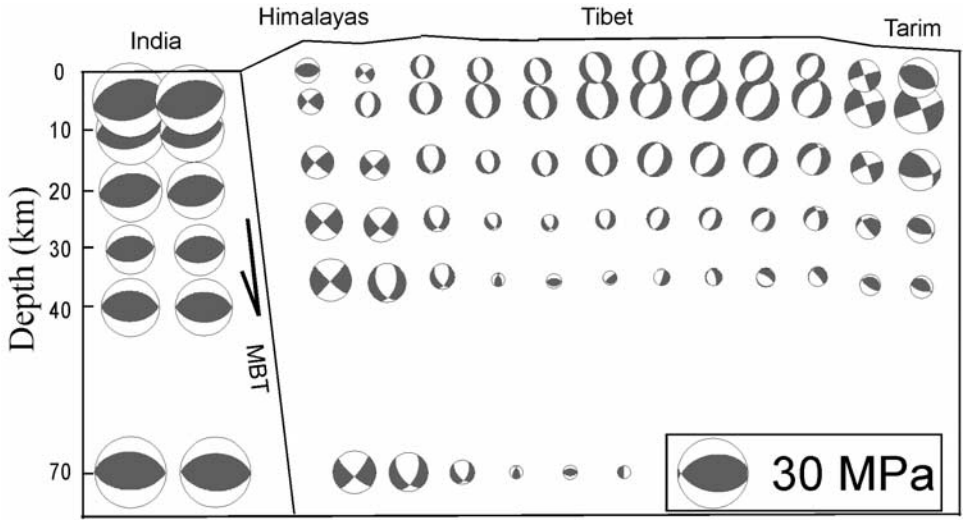

Figure 9. Vertical profile of the predicted deviatoric stresses when a stiffer lithosphere for the Himalayas and southern Tibet was assumed (viscosity values below 20 km depth were increased to $4-5 \times 10^{22}$ Pa s from 5×10^{21} Pa s, the value for the rest part of the Tibetan Plateau, see Figure 3). Note the predicted deep normal faulting under the Himalayas and southern Tibet. The stress scale is shown in the lower right corner. See color version of this figure in the HTML.

have raised questions as to the role of gravitational collapse in Tibet [*Yin*, 2000]. Although other processes may have contributed to these deep events [*Chen and Kao*, 1996; *Yin*, 2000], the role of gravitational collapse cannot be ruled out. The key factor here is lithospheric rheology: seismic data indicate that the mantle lithosphere under southern Tibet and the Himalayas is abnormally thick [*Holt and Wallace*, 1990; *McNamara et al.*, 1994], and seismic tomography shows that the high velocity structures extend as deep as 250 km [*Liu and Jin*, 1993]. Figure 9 shows that, with a relatively cold and stiff lithosphere under southern Tibet and the Himalayas, gravitational collapse may cause deep normal faulting.

4. Effects of Model Parameters and the Tectonic Implications

[15] The results presented so far indicate that the present stress field within the Tibetan crust can be explained by the combined effects of indentation of the Indian plate, gravitational spreading of the elevated plateau, and the specified boundary conditions. To better illustrate the effects of gravitational collapse, Figure 10 shows the predicted crustal stresses and surface velocity field for a case where the parameters are the same as those in Figure 6, except that a fixed (zero displacement) boundary condition is imposed on all sides of the model domain to isolate the effects of gravitational collapse. Naturally, the elevated plateau tends to spread in all directions; the spreading rates correlate with the topographic gradients, with the highest rates found near the Himalayan front (Figure 10a). The resulting stresses showing predominantly N-S extension, again because of the greatest topographic gradients in the Himalayan front and the northern margin of the Tibetan Plateau. In nature, the deformation field is altered by the indentation of the Indian plate and other factors and boundary conditions. Some of these factors and boundary conditions have been suggested as major causes of the E-W Tibetan extension. Here we explore the effects of some of these factors.

4.1. Boundary Conditions

[16] Following the Indo-Asian collision, deformation within the Tibetan Plateau has been largely confined by the Tarim block to its north and the Pamir to its west (Figure 1). The major uncertainty is the nature of the eastern boundary of the plateau, which has been relatively free through the Cenozoic, accommodating much of the collisional deformation [*Allegre et al.*, 1984; *Tapponnier and Molnar*, 1977]. At present, the eastern side of the plateau moves eastward with respect to the stable Eurasia at $\sim$15 mm yr^{-1} [*Chen et al.*, 2000]. However, the GPS velocities, measured over a period of a few years, may not fully represent the long-term averaged geological rate of crustal escape [*Liu et al.*, 2000b]. Whereas significant eastward extrusion of crustal blocks along numerous strike-slip faults may have occurred following the Indo-Asian collision, the amount of crustal translation has been uncertain. The estimated total offset along the Altyn Tagh fault, for example, range from $\sim$200 to >1000 km (see a summary by *Yin and Harrison* [2000]). Also in debate is the cause of the lateral crustal translation: in addition to the indentation of the Indian plate, the GPE of the elevated Tibetan Plateau and far-field stresses may have also contributed to the eastward crustal escaping [*Kong et al.*, 1997]. *Yin* [2000] has argued that the E-W Tibetan extension shows temporal and spatial correlations with other Cenozoic extension systems in eastern Asia, and may have resulted from the same regional extensional forces arising from plate boundary processes along the eastern margins of the Asian continent.

[17] To test this hypothesis we may impose an extensional force on the eastern side of the Tibetan Plateau to see if it is sufficient to explain the E-W extension in Tibet. However, the nature and magnitude of such far-field forces are poorly

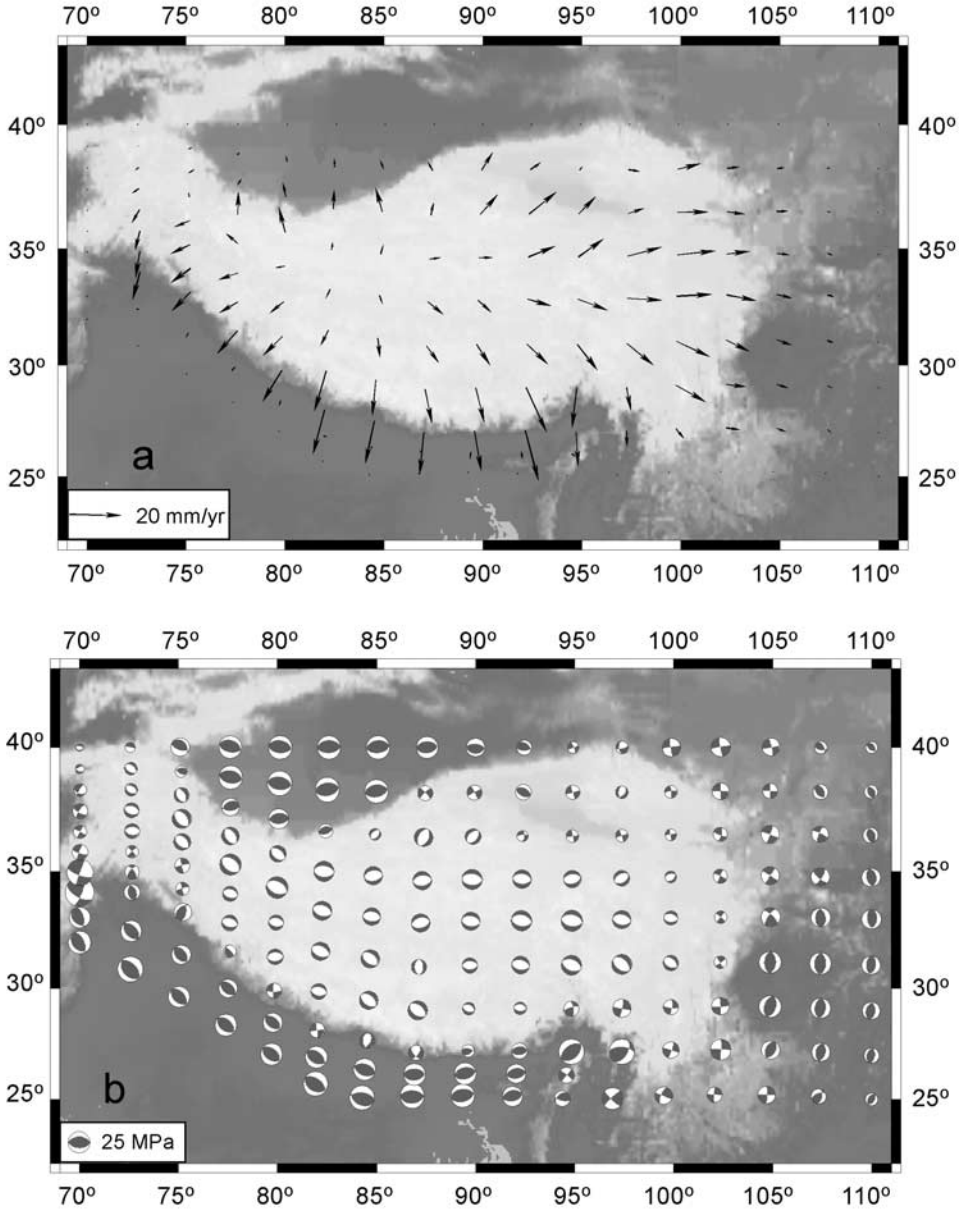

Figure 10. Effects of gravitational collapse. The fixed boundary (zero displacement) is applied to all sides of the model domain; other model parameters are the same as in Figure 6. (a) Predicted surface velocity field. (b) Predicted deviatoric stresses in the upper crust (at 10 km depth) of the Tibetan Plateau and surrounding regions. See color version of this figure in the HTML.

known. Alternatively, we tested an end-member case with no far-field extensional force acting on the eastern side of the plateau. Figure 11 shows the predicted crustal stresses in a case with other parameters being the same as in Figure 6, except that a fixed boundary (no lateral displacement) is now assumed on the eastern side of the model. A comparison with Figure 6, where a 10 mm yr^{-1} eastward velocity boundary was imposed on the eastern side of the model, shows remarkable similarity, including extensional stresses in Tibet. Such results are not surprising, considering the relative magnitude of the deviatoric stresses involved here. Let us assume that all the eastward extrusion was caused by the far-field extensional stress. For a vertically averaged effective viscosity in the range of 10^{21}–10^{22} Pa s for the Tibetan lithosphere, the horizontal stress needed to stretch the eastern side of the Tibetan Plateau at 10 mm yr^{-1} is only a few mega pascals (stress = viscosity × strain rate). The vertical stress due to topographic loading, on the other hand, is up to 150 MPa under Tibet. Thus gravitationally induced extensional stress states are expected to dominate in Tibet, with or without the far-field extensional force, although such far-field force would certainly facilitate the Tibetan crustal extension.

4.2. Basal Shear

[18] Subduction of the continental Indian plate is likely to exert considerable basal shear on the overriding Eurasian plate. Shear stresses as high as 300 MPa have been

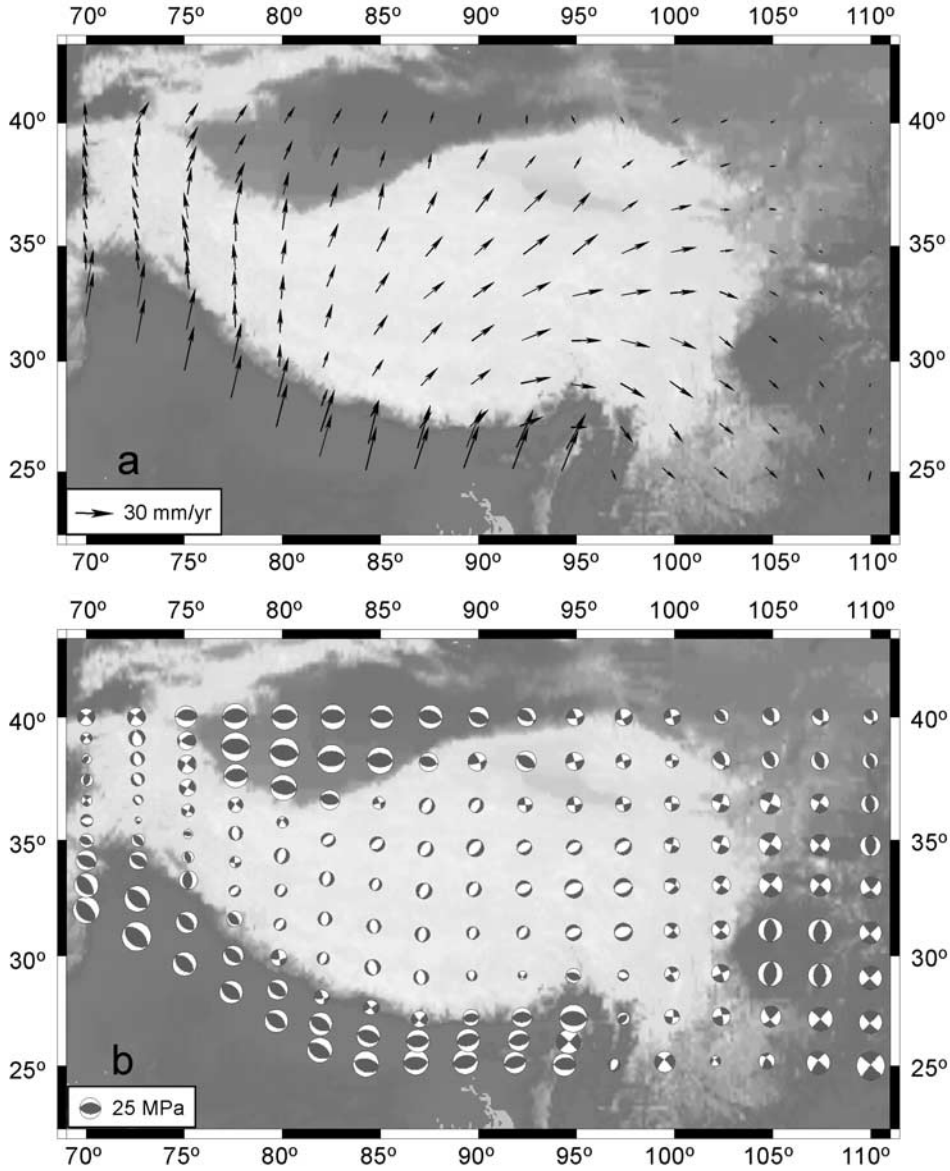

Figure 11. Effects of a fixed boundary on the eastern side of the model domain. All other model parameters are the same as in Figure 6. (a) Predicted surface velocity field. (b) Predicted deviatoric stresses in the upper crust (at 10 km depth). The similarity between this figure and Figure 6 suggest that a regional extensional force on the eastern side of the Tibetan Plateau is not required for the observed E-W extension. See color version of this figure in the HTML.

suggested based on the evidence of metamorphic petrology across the Main Central Thrust [*Molnar and England*, 1990], although recent studies suggest that the geological data can be explained by moderate shear stresses, on the order of 30 MPa or so [*Harrison et al.*, 1998b]. In some mechanical models, basal shear is considered the major driving force for the Tibetan mountain building [*Buck and Sokoutls*, 1994; *Willett et al.*, 1993; *Willett and Beaumont*, 1994]. Given the arc geometry of the Himalayan front, some authors also suggested basal shear as a major cause of the E-W extension in the Himalayas and southern Tibet [*McCaffrey and Nabelek*, 1998; *Seeber and Pecher*, 1998].

[19] We have investigated the impact of basal shear on the stress states within the Tibetan Plateau. Figure 12 shows the results of predicted crustal stresses when 10 MPa shear stress is applied to the base of the model domain south of the Indus-Zangbo suture zone (IZSZ) (Figure 1) while other parameters are the same as in Figure 6. A comparison with Figure 6 shows that, although the general stress patterns remain similar, the basal shear tends to hinder extension in the northern and central Tibetan Plateau while enhancing extension in southern Tibet and the Himalayas. The reason is that the applied basal shear reduces the compressive (indentation) stresses at the southern edge of the Tibetan Plateau needed to balance the gravitational buoyancy force of the plateau. This leads to weaker compression within the upper crust in the Himalayas and southern Tibet, thus facilitating exten-

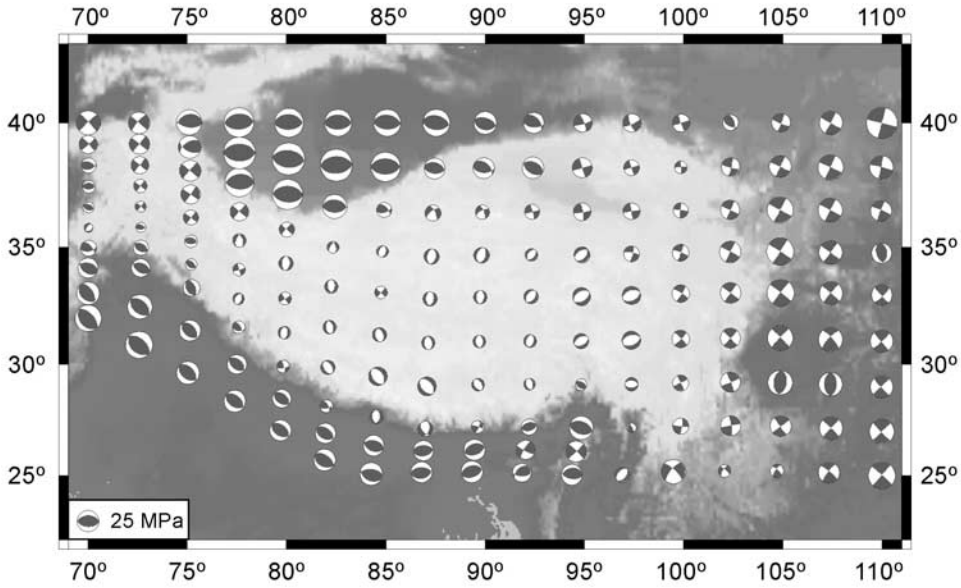

Figure 12. Predicted deviatoric stresses in the upper crust (at 10 km depth) of the Tibetan Plateau when basal shear stresses (10 MPa) are applied to the bottom of the model domain south of the IZSZ. Other parameters are the same as in Figure 6. The applied basal shear tends to enhance crustal extension in southern Tibet while hindering extension in northern Tibet (compare Figure 6). See color version of this figure in the HTML.

sion there. North of the IZSZ, the basal shear adds to the horizontal compression, thus hindering crustal extension. Although recent field studies have revealed more extensional structures in central northern Tibet than previously known [*Blisniuk et al.*, 2001; *Yin et al.*, 1999], the best developed north trending grabens are found in southern Tibet and the Himalayan front, probably reflecting the impact of basal shear.

[20] Another effect of the applied basal shear is a rotation of the predicted extensional direction from roughly E-W (Figure 6) to NE-SW (Figure 12). This change resulted from the combined effects of oblique subduction of the Indian plate and the topographic gradients in the Himalayan front. We discuss later that this mechanism may have some interesting implications for the development of the South Tibetan Detachment System (STDS) [*Burchfiel et al.*, 1992].

5. Implications for the Rise and Fall of the Tibetan Plateau

[21] The numerical model constrained by the active tectonics in Tibet may be used to gain some insights into the rise and fall of the Tibetan Plateau by exploring the model parameters and boundary conditions that may have changed significantly during the orogenic history.

5.1. The Dynamic Link Between the Rise and Fall of the Tibetan Plateau

[22] When did the Tibetan Plateau reach its present mean high elevation is a question of great importance to the Tibetan tectonics and climate change [*Harrison et al.*, 1998a; *Molnar et al.*, 1993; *Ruddiman and Kutzbach*, 1989]. Because of the difficulty of dating paleoaltitude, various proxies have been used. One approach is to date the normal faults bounding the north trending grabens in the plateau, assuming that such E-W crustal extension was caused by gravitational collapse of the plateau when it reached its present mean high elevation. By dating igneous intrusions crosscutting the normal faults, the age of the plateau reaching its present mean high elevation was estimated to be 8–14 Ma [*Coleman and Hodges*, 1995; *Edwards and Harrison*, 1997].

[23] Using a simple 3-D finite element model, *Liu et al.* [2000a] showed that the E-W Tibetan extension might have occurred at a much lower elevation. In this work we refined Liu et al.'s results with a more realistic and better constrained model. Figure 13 shows the predicted crustal stresses for a case where the elevation of the plateau is reduced by 50% while other parameters are the same as in Figure 6. In this case no E-W extension within the plateau is predicted, and strike-slip faults are the dominant features over the plateau. Significant crustal extension is predicted only when the elevation of the plateau reaches >75% of its present value. The assumption here is that the plate convergence rate and the general boundary conditions around the Tibetan Plateau did not change significantly through the late Cenozoic. There is no evidence for significant changes of the Indo-Asian convergence rate over the past 50 Myr, and our preliminary results of long-term finite strain modeling [*Liu and Yang*, 2002] suggest that tectonic boundary conditions at the early stages of the Indo-Asian collision were more favorable for lateral extrusion along strike-slip faults. Note that in Figure 13, no lateral rheologic variations within the Tibetan Plateau were considered. If preexisting weak zones within the plateau are included, as indicated by geological evidence [*Yin and Harrison*, 2000], some of the predicted strike-slip motion may be replaced by thrusting and contraction within these weak zones. These results are consistent with geological evidence of normal faulting in

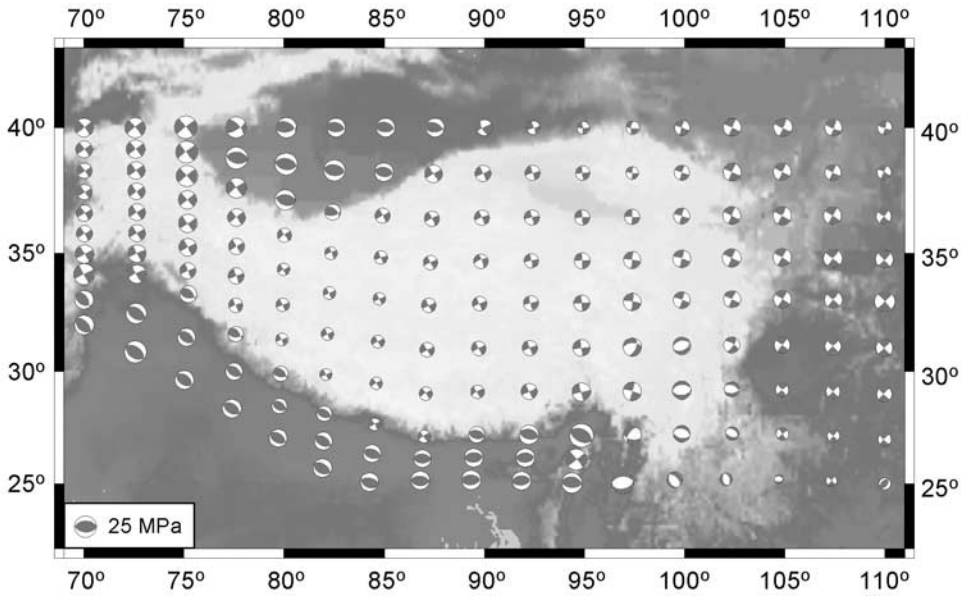

Figure 13. Predicted deviatoric stresses in the upper crust (at 10 km depth) of the Tibetan Plateau when the elevation of the Himalayas-Tibetan Plateau is reduced to half of its present value. No E-W extension is predicted in the plateau, and strike-slip motion is the predominant feature. See color version of this figure in the HTML.

Tibet occurring much later than the internal crustal shortening and the development of the major strike-slip faults [*Dewey et al.*, 1988; *Yin and Harrison*, 2000].

[24] The geological evidence for the timing of the rise of the Tibetan Plateau ranges from a few million years ago [*Zheng et al.*, 2000] to more than 40 Myr [*Chung et al.*, 1998; *Murphy et al.*, 2002]. There is also evidence for significant elevation of southern Tibet prior to the Indo-Asian collision [*Murphy et al.*, 1997]. It is possible that the uplift of the plateau is heterogeneous in space and in time. The lack of widespread, old north trending rifts in Tibet, on the other hand, suggests that the E-W Tibetan extension occurred only when most of the plateau reached some critical high elevation.

5.2. The South Tibetan Detachment System

[25] The E-W extension in the Tibetan Plateau was preceded by the development of the STDS [*Burchfiel et al.*, 1992]. The STDS is an east striking, north dipping system of normal faults that extends at least 700 km and probably through the entire 2000 km length of the northern front of the Himalayan orogen and the southernmost Tibetan Plateau. It is Miocene to perhaps Pliocene in age and contemporaneous with structurally lower south vergent thrusting within the Himalayan orogen to the south [*Burchfiel et al.*, 1992; *Burg et al.*, 1984]. These normal faults have been attributed to gravitational collapse of the elevated Himalayan front based on 2-D mechanical models [*Burchfiel and Royden*, 1985; *Royden and Burchfiel*, 1987]. Problems arise in 3-D models because extension in the direction of plate convergence is more difficult to develop than in the direction perpendicular to plate convergence [*Liu et al.*, 2000a]. If much of the Tibetan Plateau remained relatively low except for a high collisional front in the Himalayas through much of the Miocene, then a northward directed collapse of the Himalayan front may be possible, as suggested by *Burchfiel and Royden* [1985]. However, geological evidence points to high elevation (3–4 km) for at least some part of southern Tibet during the Miocene or earlier [*Murphy et al.*, 1997; *Yin et al.*, 1994]. A major drop of the compressive stresses from the collision, either due to a decelerated convergence or weak coupling between the Indian and Eurasian plates, may also contribute to the formation of the STDS. But there is no evidence of decelerated Indo-Asian convergence during the Miocene, and during that period the mechanical coupling between the convergent plates was likely strong, as indicated by the contemporaneous development of the Main Central Thrust and the MBT systems [*Burchfiel et al.*, 1992; *Hodges*, 2000], and by the formation of the Himalayan leucogranites that may have resulted from strong shear heating associated with underthrusting of the Indian plate [*England and Molnar*, 1993; *Harrison et al.*, 1998b].

[26] One interesting explanation for the STDS relates it to a southward extrusion of a crustal wedge bounded by the Main Central Thrust on the bottom and the STDS on the top [*Burchfiel et al.*, 1992; *Hodges et al.*, 1992]. The extrusion is suggested to be driven by the topographic gradient across the Himalayas, and facilitated by a thermally weakened midcrust. However, it remains unclear (1) why the north directed normal faulting did not continue to present and (2) how the STDS is related to the younger E-W extension.

[27] Both field observation and our model results indicate that E-W extension is the predominant stress state under the present tectonic conditions. The development of the STDS thus indicates different tectonic conditions during the Miocene; one such condition was likely a strong basal shear associated with the subduction of the Indian plate. We have shown (Figure 12) that increasing the basal shear would relieve the indentation stresses acting on the southern edge of the Asian continent, thus reducing the compressive

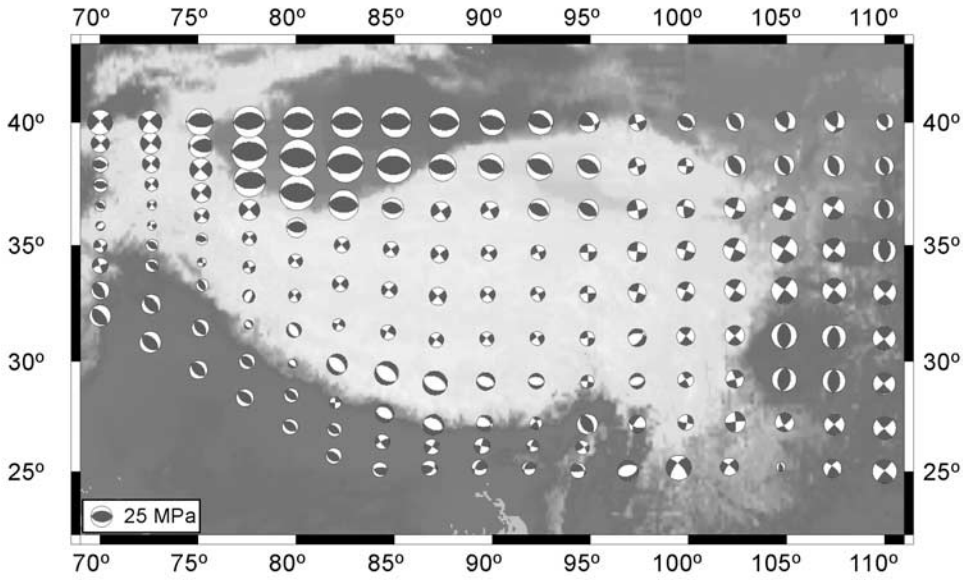

Figure 14. Predicted deviatoric stresses in the upper crust (at 10 km depth) of the Tibetan Plateau when 30 MPa basal shear stresses are applied to the bottom of the model domain south of the IZSZ. Other parameters are the same as in Figure 6. Note the nearly N-S extension confined to Himalayan front. This mechanism may help to explain the development of the South Tibetan Detachment System. See color version of this figure in the HTML.

stresses within the upper crust of the Himalayas and southern Tibet. Figure 14 shows the predicted stress pattern in the upper crust when a 30-MPa shear stress was applied to the base of the model domain south of the IZSZ. A comparison with Figures 6 and 12 shows that the increased basal shear tends to narrow the zone of crustal extension to southern Tibet and the Himalayas, while the direction of extension is rotated from E-W (Figure 6) to roughly N-S (Figure 14). The predicted narrow belt of N-S extension is consistent with the occurrence of the STDS, and a strong basal shear during the Miocene would be consistent with the development of the MCT and the associated leucogranites in mid-Miocene [*Hodges et al.*, 1988]. This mechanism could complement the model of crustal wedge extrusion [*Burchfiel et al.*, 1992; *Hodges et al.*, 1992]: The reduced compressive stresses in the upper middle crust would facilitate the southward extrusion of the crustal wedge driven by topographically induced pressure gradient. We remind the readers that Figure 14 shows the deviatoric stresses within the upper crust. Stresses near the base of the crust can be significantly different, especially when basal shear is applied.

6. Conclusions

[28] Although numerous factors may have contributed to the crustal extension in the Himalayan-Tibetan Plateau, their relative roles are often debated. We have evaluated the roles of excessive GPE, basal shear, rheologic structure, far-field force, and local boundary conditions in the rise and fall of the Himalayan-Tibetan Plateau using a 3-D finite element model. Major conclusions that we may draw from this study include the following:

[29] 1. The present crustal deformation in the Himalayan-Tibetan Plateau reflects a mechanical balance between the gravitational buoyancy force of the plateau, the indenting Indian plate, and the specific geometry and boundary conditions around the plateau. The predominately E-W extension in the past 10 Myr or so can be largely explained by gravitational collapse of the plateau. Far-field extensional forces would have enhanced the crustal extension but are not required.

[30] 2. Significant E-W Tibetan extension occurred when the Himalayan-Tibetan Plateau reached >75% of its present mean high elevation. Although the uplift history of the plateau may be heterogeneous in time and space, the occurrence of widespread north trending rifts in the plateau in the past 10–15 Myr or so suggest that only since that time did the entire plateau reached the present mean high elevation. Strike-slip faulting and eastward escaping dominated in the early stages of the Himalayan-Tibetan oreogesis.

[31] 3. The present E-W extension in Tibet constrains the effective viscosity for long-term deformation of the Tibetan crust to be in the range of 10^{21}–10^{22} Pa s, similar to the estimations of previous studies. However, rock rheology is timescale dependent, thus caution is needed when combining observational data that represent different timescales. Over the short terms pertinent to most GPS measurements, crustal deformation is close to that of elastic or elastic-plastic media. The surface velocity field in Tibet predicted in a model assuming an elastic crust is consistent with the GPS data.

[32] 4. Basal shear associated with the subduction of the Indian plate under Tibet tends to enhance crustal extension in the Himalayas and southern Tibet while increase crustal compression in northern Tibet. A moderate basal shear south of the Indus-Zangbo suture may have contributed to the relatively better developed north trending grabens in southern Tibet and the Himalayas. A strong basal shear

(~30 MPa) during the Miocene may be responsible for the development of the STDS by releasing compressive stresses on the southern edge of the Asian continent.

[33] **Acknowledgments.** We thank An Yin, John Nabelek, Bill Holt, and Eric Sandvol for helpful discussions. Comments by Jean Braun (AE) and two anonymous reviewers improved the paper. This work was supported by NSF grants EAR-9805127 and EAR-0207200, NASA NAG5-9145, the Research Board of the University of Missouri system, and the Research Council of the University of Missouri-Columbia.

References

Allegre, C. J., et al., Structure and evolution of the Himalaya-Tibet orogenic belt, *Nature*, *307*, 17–22, 1984.

Armijo, R., P. Tapponnier, J. L. Mercier, and T. L. Han, Quaternary extension in southern Tibet: Field observations and tectonic implications, *J. Geophys. Res.*, *91*, 13,803–13,872, 1986.

Artyushkov, E. V., Stresses in the lithosphere caused by crustal thickness inhomogeneities, *J. Geophys. Res.*, *78*, 7675–7690, 1973.

Bird, P., Lateral extension of lower crust from under high topography in the isostatic limit, *J. Geophys. Res.*, *96*, 10,275–10,286, 1991.

Blisniuk, P. M., B. R. Hacker, J. Glodny, L. Ratschbacher, S. Bi, Z. Wu, M. O. McWilliams, and A. Calvert, Normal faulting in central Tibet since at least 13.5 Myr ago, *Nature*, *412*, 628–632, 2001.

Brace, W. F., and D. L. Kohlstedt, Limits on lithospheric stress imposed by laboratory experiments, *J. Geophys. Res.*, *85*, 6248–6252, 1980.

Buck, W. R., and D. Sokoutls, Analogue model of gravitational collapse and surface extension during continental convergence, *Nature*, *369*, 737–740, 1994.

Burchfiel, B. C., and L. H. Royden, North-south extension within the convergent Himalayan region, *Geology*, *13*, 679–682, 1985.

Burchfiel, B. C., Z. Chen, K. V. Hodges, Y. Liu, L. H. Royden, C. Deng, and J. Xu, The South Tibetan detachment system, Himalayan orogen: Extension contemporaneous with and parallel to shortening in a collisional mountain belt, *Spec. Pap. Geol. Soc. Am.*, *269*, 41 pp., 1992.

Burg, J. P., M. Brunel, D. Gapais, G. M. Chen, and G. H. Liu, Deformation of leucogranites of the crystalline Main Central Thrust sheet in southern Tibet (China), *J. Struct. Geol.*, *6*, 535–542, 1984.

Chen, W.-P., and H. Kao, Seismotectonics of Asia: Some recent progress, in *The Tectonic Evolution of Asia*, edited by A. Yin and M. Harrison, pp. 37–62, Cambridge Univ. Press, New York, 1996.

Chen, W.-P., and P. Molnar, Focal depths of intracontinental and intraplate earthquakes and their implications for the thermal and mechanical properties of the lithosphere, *J. Geophys. Res.*, *88*, 4183–4214, 1983.

Chen, Z., B. C. Burchfiel, Y. Liu, R. W. King, L. H. Royden, W. Tang, E. Wang, J. Zhao, and X. Zhang, Global positioning system measurements from eastern Tibet and their implications for India/Eurasia intercontinental deformation, *J. Geophys. Res.*, *105*(7), 16,215–16,227, 2000.

Chung, S. L., C. H. Lo, T. Y. Lee, Y. Zhang, Y. Xie, X. Li, K. L. Wang, and P. L. Wang, Diachronous uplift of the Tibet Plateau starting 40 Myr ago, *Nature*, *394*, 769–773, 1998.

Coleman, M., and K. Hodges, Evidence for Tibetan Plateau uplift before 14 Myr ago from a new minimum age for east-west extension, *Nature*, *374*, 49–52, 1995.

DeMets, C., R. G. Gordon, D. F. Argus, and S. Stein, Effect of recent revisions to the geomagnetic reversal time scale on estimates of current plate motion, *Geophys. Res. Lett.*, *21*, 2191–2194, 1994.

Desai, C. S., *Elementary Finite Element Method*, 434 pp., Prentice-Hall, Old Tappan, N. J., 1979.

Dewey, J. F., Extensional collapse of orogens, *Tectonics*, *7*, 1123–1139, 1988.

Dewey, J. F., R. M. Shackleton, C. Chang, and Y. Sun, The tectonic evolution of the Tibetan Plateau, *Philos. Trans. R. Soc. London, Ser. A*, *327*, 379–413, 1988.

Edwards, M. A., and T. M. Harrison, When did the roof collapse? Late Miocene north-south extension in the high Himalaya revealed by Th-Pb monazite dating of the Khula Kangri granite, *Geology*, *25*, 543–546, 1997.

England, P., and G. Houseman, The mechanics of the Tibetan Plateau, *Philos. Trans. R. Soc. London, Ser. A*, *327*, 379–413, 1988.

England, P., and P. Molnar, Active deformation of Asia: From kinematics to dynamics, *Science*, *278*, 647–650, 1997.

England, P. C., and G. A. Houseman, Finite strain calculations of continental deformation, 2, Comparison with the India-Asia collision, *J. Geophys. Res.*, *91*, 3664–3676, 1986.

England, P. C., and G. A. Houseman, Extension during continental convergence with special reference to the Tibetan Plateau, *J. Geophys. Res.*, *94*, 17,561–17,597, 1989.

England, P. C., and D. P. McKenzie, A thin viscous sheet model for continental deformation, *Geophys. J. R. Astron. Soc.*, *70*, 295–321, 1982.

England, P. C., and P. Molnar, The interpretation of inverted metamorphic isograds using simple physical calculations, *Tectonics*, *12*, 145–157, 1993.

Flesch, L. M., W. E. Holt, A. J. Haines, and T. B. Shen, Dynamics of the Pacific-North American plate boundary in the western United States, *Science*, *287*(5454), 834–836, 2000.

Flesch, L. M., A. J. Haines, and W. E. Holt, Dynamics of the India-Eurasia collision zone, *J. Geophys. Res.*, *106*, 16,435–16,460, 2001.

Goodman, R. E., R. L. Taylor, and T. L. Brekke, *A Model for the Mechanics of Jointed Rock*, pp. 637–659, Am. Soc. of Civ. Eng., New York, 1968.

Guo, Z. T., W. F. Ruddiman, Q. Z. Hao, H. B. Wu, Y. S. Qiao, R. X. Zhu, S. Z. Peng, J. J. Wei, B. Y. Yuan, and T. S. Liu, Onset of Asian desertification by 22 Myr ago inferred from loess deposits in China, *Nature*, *416*, 159–163, 2002.

Harrison, M., A. Yin, and F. J. Ryerson, Orographic evolution of the Himalaya and Tibetan Plateau, in *Tectonic Boundary Conditions for Climate Reconstruction*, edited by T. J. Crowley and K. C. Burke, pp. 21–71, Oxford Univ. Press, New York, 1998a.

Harrison, T. M., M. Grove, O. M. Lovera, and E. J. Catlos, A model for the origin of Himalayan anatexis and inverted metamorphism, *J. Geophys. Res.*, *103*, 27,017–27,032, 1998b.

Hodges, K. V., Tectonics of the Himalaya and southern Tibet from two perspectives, in *Special Focus on the Himalaya*, edited by J. W. Geissman and A. F. Glazner, Geol. Soc. of Am., Boulder, Colo., 2000.

Hodges, K. V., M. S. Hubbard, D. S. Silverberg, Metamorphic constraints on the thermal evolution of the central Himalayan orogen, in *Tectonic Evolution of the Himalayas and Tibet*, pp. 257–280, R. Soc. of London, London, 1988.

Hodges, K. V., R. R. Parrish, T. B. Housh, D. R. Lux, B. C. Burchfiel, L. H. Royden, and Z. Chen, Simultaneous Miocene extension and shorting in the Himalayan orogen, *Science*, *258*, 1466–1470, 1992.

Holt, W., and T. C. Wallace, Crustal thickness and upper mantle velocities in the Tibetan Plateau region from the inversion of regional *Pnl* waveforms: Evidence for a thick upper mantle lid beneath southern Tibet, *J. Geophys. Res.*, *95*, 12,499–12,525, 1990.

Houseman, G., and P. England, A lithospheric-thickening model for the Indo-Asian collision, in *The Tectonic Evolution of Asia*, edited by A. Yin and T. M. Harrision, pp. 3–17, Cambridge Univ. Press, New York, 1996.

Kirby, S. H., and A. K. Kronenberg, Rheology of the lithosphere: Selected topics, *Rev. Geophys.*, *25*, 1219–1244, 1987.

Kong, X., A. Yin, and T. M. Harrison, Evaluating the role of preexisting weakness and topographic distributions in the Indo-Asian collision by use of a thin-shell numerical model, *Geology*, *25*, 527–530, 1997.

Kutzbach, J. E., P. J. Guetter, W. F. Ruddiman, and W. L. Prell, Sensitivity of climate to late Cenozoic uplift in southern Asia and the American West; numerical experiments, *J. Geophys. Res.*, *94*, 18,393–18,407, 1989.

Larson, K., R. Burgmann, R. Bilham, and J. T. Freymueller, Kinematics of the India-Eurasia collision zone from GPS measurements, *J. Geophys. Res.*, *104*, 1077–1094, 1999.

Liu, F., and A. Jin, Seismic tomography of China, in *Seismic Tomography: Theory and Practice*, edited by H. M. Iyer and K. Hirahara, pp. 299–310, Chapman and Hall, New York, 1993.

Liu, M., and Y. Shen, Crustal collapse, mantle upwelling, and Cenozoic extension in the North American Cordillera, *Tectonics*, *17*, 311–321, 1998.

Liu, M., and Y. Yang, Crustal thickening and lateral extrusion during the formation of the Tibetan Plateau: Insights from 3-D numerical modeling, *Eos Trans AGU*, *83*(47), Fall Meet. Suppl., Abstract S61D-04, 2002.

Liu, M., Y. Shen, and Y. Yang, Gravitational collapse of orogenic crust: A preliminary three-dimensional finite element study, *J. Geophys. Res.*, *105*, 3159–3173, 2000a.

Liu, M., Y. Yang, S. Stein, Y. Zhu, and J. Engeln, Crustal shortening in the Andes: Why do GPS rates differ from geological rates?, *Geophys. Res. Lett.*, *27*, 3005–3008, 2000b.

Liu, M., Y. Yang, S. Stein, and E. Klosko, Crustal shortening and extension in the central Andes: Insights from a viscoelastic model, in *Plate Boundary Zones*, *Geodyn. Ser.*, vol. 30, edited by S. Stein and J. T. Freymueller, pp. 325–339, AGU, Washington, D. C., 2002.

McCaffrey, R., and J. Nabelek, Role of oblique convergence in the active deformation of the Himalayas and southern Tibet plateau, *Geology*, *26*, 691–694, 1998.

McNamara, D. E., T. J. Owens, P. G. Silver, and F. T. Wu, Shear wave anisotropy beneath the Tibetan Plateau, *J. Geophys. Res.*, *99*, 13,655–13,666, 1994.

Mercier, J. L., R. Armijo, P. Tapponnier, E. Carey-Gailhardis, and T. Han, Change from Tertiary compression to Quaternary extension in southern Tibet during the India-Asia collision, *Tectonics*, *6*, 275–304, 1987.

Molnar, P., and W. P. Chen, Focal depths and fault plane solutions of earthquakes under the Tibetan Plateau, *J. Geophys. Res.*, *88*, 1180–1196, 1983.

Molnar, P., and P. England, Temperatures, heat flux, and frictional stress near major thrust faults, *J. Geophys. Res.*, *95*, 4833–4856, 1990.

Molnar, P., and H. Lyon-Caen, Some simple physical aspects of the support, structure, and evolution of mountain belts, *Spec. Pap. Geol. Soc. Am.*, *218*, 179–207, 1988.

Molnar, P., and P. Tapponnier, Relation of the Tectonics of eastern China to the India-Eurasia collision: Application of slip-line field theory to large-scale continental tectonics, *Geology*, *5*, 212–216, 1977.

Molnar, P., P. England, and J. Martinod, Mantle dynamics, uplift of the Tibetan Plateau, and the Indian monsoon, *Rev. Geophys.*, *31*, 357–396, 1993.

Murphy, M. A., A. Yin, T. M. Harrision, S. B. Durr, Z. Chen, F. J. Ryerson, W. S. F. Kidd, X. Wang, and X. Zhou, Did the Indo-Asian collision alone create the Tibetan Plateau?, *Geology*, *25*, 719–722, 1997.

Murphy, M. A., A. Yin, P. Kapp, T. M. Harrison, C. E. Manning, F. J. Ryerson, L. Ding, and J. Guo, Structural evolution of the Gurla Mandhata detachment system, Southwest Tibet; implications for the eastward extent of the Karakoram fault system, *Geol. Soc. Am. Bull.*, *114*, 428–447, 2002.

Ni, J., and J. E. York, Late Cenozoic tectonics of the Tibet Plateau, *J. Geophys. Res.*, *83*, 5377–5387, 1978.

Paul, J., et al., The motion and active deformation of India, *Geophys. Res. Lett.*, *28*, 647–650, 2001.

Ratschbacher, L., W. Frisch, G. Liu, and C. Chen, Distributed deformation in southern and western Tibet during and after the India-Asia collision, *J. Geophys. Res.*, *99*, 19,917–19,946, 1994.

Royden, L., Coupling and decoupling of crust and mantle in convergent orogens: Implications for strain partitioning in the crust, *J. Geophys. Res.*, *101*, 17,679–17,705, 1996.

Royden, L. H., and B. C. Burchfiel, Thin skinned N-S extension within the convergent Himalaya region: Gravitational collapse of a Miocene topographic front, in *Continental Extensional Tectonics*, edited by M. P. Coward, J. F. Dewey, and P. L. Hancock, *Geol. Soc. Spec. Publ.*, *28*, 611–619, 1987.

Ruddiman, W. F., and J. E. Kutzbach, Forcing of late Cenozoic Northern Hemisphere climate by plateau uplift in southern Asia and the American west, *J. Geophys. Res.*, *94*, 18,409–18,427, 1989.

Seeber, L., and A. Pecher, Strain partitioning along the Himalayan arc and the Nanga Parbat antiform, *Geology*, *26*, 791–794, 1998.

Tapponnier, P., and P. Molnar, Active faulting and tectonics in China, *J. Geophys. Res.*, *82*, 2905–2930, 1977.

Tapponnier, P., J. L. Mercier, R. Armijo, T. Han, and J. Zhou, Field evidence for active normal faulting in Tibet, *Nature*, *294*, 410–414, 1981.

Wang, Q., et al., Present-day crustal deformation in China constrained by Global Positioning System measurements, *Science*, *294*(5542), 574–577, 2001.

Willett, S., C. Beaumont, and P. Fullsack, Mechanical model for the tectonics of double vergent compressional orogens, *Geology*, *21*, 371–374, 1993.

Willett, S. D., and C. Beaumont, Subduction of Asian lithospheric mantle beneath Tibet inferred from models of continental collision, *Nature*, *369*, 642–645, 1994.

Williams, C. A., and R. M. Richardson, A rheological layered three-dimensional model of the San Andreas Fault in central and southern California, *J. Geophys. Res.*, *96*, 16,597–16,623, 1991.

Yin, A., Mode of Cenozoic east-west extension in Tibet suggesting a common origin of rifts in Asia during the Indo-Asian collision, *J. Geophys. Res.*, *105*, 21,745–21,759, 2000.

Yin, A., and M. Harrison, Geological evolution of the Himalayan-Tibetan orogen, *Annu. Rev. Earth Planet. Sci.*, *28*, 211–280, 2000.

Yin, A., T. M. Harrison, F. J. Ryerson, C. Wenji, W. S. F. Kidd, and P. Copeland, Tertiary structural evolution of the Gangdese thrust system, southeastern Tibet, *J. Geophys. Res.*, *99*, 18,175–18,202, 1994.

Yin, A., P. A. Kapp, M. A. Murphy, C. E. Manning, T. M. Harrison, M. Grove, L. Ding, X. Deng, and C. Wu, Significant late Neogene east-west extension in northern Tibet, *Geology*, *27*, 787–790, 1999.

Zhao, W., and W. J. Morgan, Injection of Indian crust into Tibetan lower crust: A two-dimensional finite element model study, *Tectonics*, *6*, 489–504, 1987.

Zheng, H., C. M. Powell, Z. An, J. Zhou, and G. Dong, Pliocene uplift of the northern Tibetan Plateau, *Geology*, *28*, 715–718, 2000.

Zhisheng, A., J. E. Kutzbach, W. L. Prell, and S. C. Porter, Evolution of Asian monsoons and phased uplift of the Himalaya-Tibetan Plateau since late Miocene times, *Nature*, *411*, 62–66, 2001.

M. Liu and Y. Yang, Department of Geological Sciences, University of Missouri-Columbia, 101 Geology Building, Columbia, MO 65211, USA. (lium@missouri.edu)